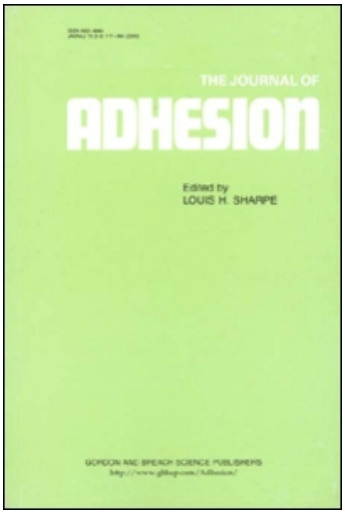

The Journal of Adhesion
Publication details, including instructions for authors and subscription information:
http://www.informaworld.com/smpp/title~content=t713453635

Surface Preparation of Ti-6Al-4V for High-Temperature Adhesive Bonding

H. M. Clearfield[a]; D. K. Shaffer[a]; S. L. Vandoren[a]; J. S. Ahearn[a]
[a] Martin Marietta Laboratories, Baltimore, MD, U.S.A.

To cite this Article Clearfield, H. M. , Shaffer, D. K. , Vandoren, S. L. and Ahearn, J. S.(1989) 'Surface Preparation of Ti-6Al-4V for High-Temperature Adhesive Bonding', The Journal of Adhesion, 29: 1, 81 — 102
To link to this Article: DOI: 10.1080/00218468908026479
URL: http://dx.doi.org/10.1080/00218468908026479

J. Adhesion, 1989, Vol. 29, pp. 81–102
Reprints available directly from the publisher
Photocopying permitted by license only

Printed in the United Kingdom

Surface Preparation of Ti-6Al-4V for High-Temperature Adhesive Bonding†

H. M. CLEARFIELD, D. K. SHAFFER, S. L. VANDOREN and J. S. AHEARN

Martin Marietta Laboratories, 1450 S. Rolling Road, Baltimore, MD 21227, U.S.A.

(Received October 5, 1988; in final form November 28, 1988)

The role of surface preparation in high-temperature bond durability is investigated for Ti-6Al-4V adherends. Four surface preparations, including a newly-introduced treatment, plasma-sprayed Ti-6Al-4V coatings, are evaluated using a simple tensile test and a wedge/crack-propagation test. At temperatures approaching 300°C, the oxide-metal interface of oxide preparations becomes unstable. Such exposure results in a weakening of the oxide and, hence, bond failure at low tensile strength. The plasma-sprayed coating is a microscopically-rough metallic film with only a thin, native oxide. The plasma-sprayed adherend remains strong over prolonged, high-temperature exposures, and the micro-roughness is important for crack arrest in the wedge test.

KEY WORDS Titanium adhesive bonding; high service temperature adherends; metallic surface preparation; plasma sprayed coatings; durability; oxide stability.

1 INTRODUCTION

The use of adhesively-bonded structures for high service temperatures has been limited in the past due to a lack of suitably stable materials. Much research has been performed to obtain organic resins with high temperature stability and, in fact, impressive results have been obtained—up to tens of thousands of hours at 232°C with polyimides.[1,2] Very little attention has been paid to the durability of surface preparations for one of the candidate adherends, Ti-6Al-4V.[2,3] In this paper, we present an investigation of the role of surface preparation in high-temperature bond durability. Three traditional titanium surface preparations are examined, and a new one, plasma-sprayed coatings of the Ti-6Al-4V alloy, is introduced. As we will show, the plasma-sprayed coating exhibits a microscopically-rough morphology and bond durability that is projected to exceed that of the other treatments under extreme environmental conditions.

Titanium alloys have traditionally been prepared for adhesive bonding by forming an oxide at the adherend surface.[2–21] This can be achieved by anodizing

† Presented at the 35th Sagamore Army Materials Research Conference, Manchester, New Hampshire, U.S.A., June 26–30, 1988.

in acidic[2,4–12] or basic[2,13–15] media, or by etching.[7,9,10,16–20] In the case of air-formed oxides, silane coupling agents have been used for surface preparation.[21] Durability studies conducted in moderate environments, *i.e.*, 60°C and 95% relative humidity, have shown that stable, microscopically rough oxides provide the best overall performance in both tension and shear test modes.[7,9,10,13,15] The most common processes for achieving porous oxides are chromic acid anodization (CAA) and sodium hydroxide anodization (SHA). Both processes yield rather thick oxides (hundreds of Angstroms). At higher temperatures, *e.g.*, 232°C, a thinner oxide such as that formed by etching in Pasa Jell 107 (PJ)[22] seems to provide excellent durability.[2,3,6,23]

In earlier studies,[2,3,11,24] it was shown that CAA-treated Ti-6Al-4V adherends failed when exposed to high temperatures. In our specific case,[11,24] the bond strength (tensile) test was conducted after exposure of the bare adherend in air (330°C, 160–1200 hr) or vacuum (400°C, 24–160 hr). We identified the locus of failure as the oxide-metal interface and proposed that a microstructural change in the alloy was responsible for the loss in bond strength. Subsequent work, presented here, shows that a more plausible explanation is a dissociation of the oxide with subsequent diffusion or dissolution of oxygen into the alloy. This process takes place for both CAA and SHA adherends. For PJ adherends, oxygen dissolution also occurs, but is accompanied by an increase in oxide thickness.

In order to overcome the instability of the oxide-metal interface and produce a microscopically-rough surface suitable for bonding, we have used a plasma-sprayed coating of Ti-6Al-4V on the substrate surface. In plasma spraying, an electric arc is struck between a cathode and an anode (nozzle), both of which are water cooled. Working gas, typically a mixture of argon and hydrogen (or nitrogen and hydrogen), is forced through the arc, creating a plasma. A powder of the material to be deposited (in our case Ti-6Al-4V) is injected into the plasma either within or externally downstream from the nozzle. The plasma either melts or sufficiently softens the powder particles in flight, *i.e.*, while being propelled toward the substrate by the high velocity gas (plasma) flow.

Plasma-sprayed titanium and titanium alloys typically are used as coatings for corrosion resistance in chemical plant[25] or marine[26] environments, for frictional wear resistance,[27] or for promoting attachment of bone to orthopedic implants.[28] Although the application usually dictates that the coating be as free of porosity as possible, in the bone grafting study cited an intentionally porous coating allowed bone matter to infuse in, which yielded acceptable bond strength. In that case, it was suggested that the bone cement could be eliminated since bone would bond directly to the coating. Kinloch has attempted to use plasma spray coatings for preparation of steel surfaces,[29] but concluded that they were of little benefit.

In this study, we introduce the use of plasma-sprayed Ti-6Al-4V coatings for high-temperature bonding applications. As in the earlier studies, the tensile test is used to demonstrate the improvement of the technique over anodization for high-temperature applications. In addition, a durability test (wedge/crack propagation) has been conducted and the results demonstrate the need for microroughness in the coating.

II EXPERIMENTAL

A. Surface preparation and bare adherend exposure

The anodization procedures are described in detail elsewhere.[30] Briefly, Ti-6Al-4V coupons ($2 \times 5 \times 0.08$ cm or $2 \times 5 \times 0.28$ cm) are degreased in dichloromethane, pickled in a solution containing HNO_3 and HF, rinsed, anodized, rinsed again, and dried with forced hot air. For anodization, the CAA solution consists of 5% CrO_3 + 0.1% NH_4HF_2 (10 V, 25°C, 20 min) and the SHA solution is 5.0 M NaOH (10 V, 30°C, 30 min). Pasa Jell 107-treated adherends were prepared by the same degreasing and pickling procedures, followed by immersion in a solution of Pasa Jell for 20 min or application of the paste with Scotchbrite,[31] rinsing, and drying. The adherend surfaces were not protected from the laboratory ambient during transfer to the vacuum furnace or to the analytical chambers. Bonding was usually accomplished within four hours of preparation or exposure (see below).

Preparation of plasma-sprayed adherends was slightly different. After degreasing, the coupons were grit blasted with 120-mesh alumina grit. The specimens were heated prior to deposition by passing the plasma torch once over the surface. Adherends were sprayed in the laboratory ambient with Ti-6Al-4V powder to a nominal coating thickness of 50 μm. A schematic diagram of the plasma torch, which is mounted on a computer-controlled six-axis, articulated arm robot, is shown in Figure 1. This arrangement provides excellent uniformity of the coating.

Following surface preparation, some coupons were immediately placed (*i.e.*, without bonding) in a diffusion-pumped, quartz vacuum furnace with external radiant heating for 1–165 hr at temperatures from 300–900°C and at a nominal pressure of 3×10^{-4} Pa. Although the furnace was not equipped with a residual gas analyzer, the partial pressure of oxygen is estimated to be approximately 5×10^{-5} Pa.[32] Any residual water vapor in the furnace was pumped away during warmup. Furnace temperatures were monitored by a thermocouple placed at the center of the quartz tube. Because of temperature variation along the length of the tube, the temperatures reported here are nominal. Some of the coupons were heated in an ordinary laboratory furnace at 330°C for up to 1200 hr. The relative humidity of the furnace was not determined. Exposed adherends were allowed to

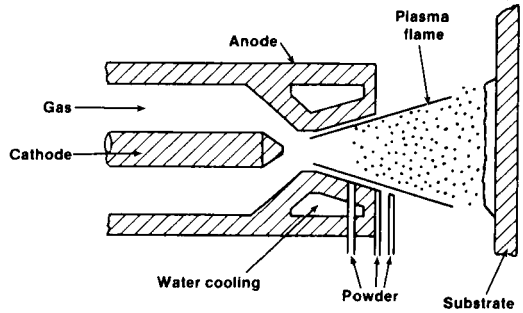

FIGURE 1 Schematic diagram of the plasma torch used in producing the plasma-sprayed Ti-6Al-4V adherends.

cool to room temperature prior to their withdrawal from the test environment and subsequent bonding.

B. Surface analysis

The adherend surfaces were analyzed by high-resolution scanning electron microscopy (SEM), X-ray photoelectron spectroscopy (XPS), and scanning Auger microscopy (SAM). A JEOL JEM 100-CX STEM, operated in the SEM mode, provided the resolution needed to examine the morphologies of the adherend oxides and the bond failure surfaces. Specimens to be examined were cut to 1.0×0.2 cm and coated with ~5 nm of Pt prior to the analysis. All stereo micrographs shown in this study were obtained at ±7 deg tilt.

The XPS measurements were made in an SSI SSX-100-03 instrument equipped with a differentially pumped sputter ion gun. The analyzer was operated at pass energies of 150 eV for overall compositional analysis or 50 eV for high-resolution analysis. These conditions correspond to a full width at half maximum of 1.4 and 0.9 eV, respectively, for the Au $4f_{7/2}$ transition. The analyzed areas were ~600 μm in diameter. Some sputter-depth profiles were obtained from a 300 μm-diameter area; however, due to difficulties with the experimental geometry for SHA adherends (see below), most of the sputter-depth profiles were obtained in the SAM.

The Auger analysis was conducted in a JEOL JAMP-10SP SAM that was also equipped with a differentailly-pumped ion gun. Because the SHA surfaces exhibited macroscopic roughness, it was important to choose an experimental geometry in which the analysis area was not shadowed from the (incident) electron beam, ion etching beam, or cylindrical mirror analyzer (CMA).[33] This was accomplished by tilting the specimen so that surface normal was at 30 deg with respect to the incident electron beam and 60 deg with respect to the CMA axis (18 deg from the cone of acceptance), and conducting the analysis in the flat areas between the macroscopic features. In order to obtain the precise focus needed for the analysis, the incident current was kept at approximately 10 nA. The CMA was operated at a modulation voltage of 5 V peak-to-peak and the etching rate for the sputter-depth profiles was calibrated by cross-sectional transmission electron microscopy (TEM) of a CAA oxide.[30]

C. Bond testing

Two types of tests were used to measure the bond strength of the (exposed) adherend surfaces and the bond durability. The relative bond strength was measured with a simple, pneumatic tensile test apparatus that has been described earlier.[11] Briefly, a 1.27-cm-diameter Al fixture is bonded to the adherend surface with a room-temperature curing epoxy (3M 1838). The tensile force is applied normal to the adherend surface, and the force required to remove the fixture is measured. Subsequently, the failure surfaces are examined by SEM and XPS to determine the locus of failure. A similar test has been used by Chaze *et al.* to

measure the adherence of thermally-grown oxides on various titanium alloys,[34] although they did not determine the locus of failure.

Wedge/crack-propagation tests were used for the bond durability studies. Surface preparation of the Ti-6Al-4V adherends ($15.2 \times 15.2 \times 0.32$ cm) was identical to that for the tensile tests. The panels were bonded with FM-300M adhesive (American Cyanamid) and cut into individual specimens (2.5×15.2 cm). A 0.3 cm wedge was used to stress the specimens, which were then immersed in distilled water at 95–100°C, thereby providing an environment severe enough to cause morphological changes in the (bare) adherend oxide.[11,35] Crack propagation prior to immersion was always in the adhesive. Following the test, the adherends were separated by driving a wedge at the opposite end (with crack propagation again in the adhesive) and the failure surfaces were examined.

III RESULTS AND DISCUSSION

A. Oxide adherend morphology and bond strength tests

The morphologies of the three oxide surfaces are shown in Figure 2. The CAA morphology (seen in Figures 2a and b) is identical to that reported previously.[3,5,6,12,35] It consists of a multilevel, honeycomb-like structure with cell diameters of ~40 nm. Cross-sectional TEM reveals that the oxide is 130-nm thick (30-nm barrier layer with 100-nm cells) and amorphous.[30] The multilevel morphology is the result of differential etching rates for the two phases of the alloy.

The SHA morphology varies with anodization temperature, time, and solution strength. The morphology obtained under the conditions described in Section II is shown in Figures 2c and d. It consists of large, mountain-like features and relatively flat areas in between that range from 0.5 to 5 μm in diameter. At high magnification, micro-roughness is evident but is distinct from that obtained by CAA. It is similar to that obtained by etching with an alkaline-peroxide solution.[10] Filbey *et al.*[14] have reported a macroscopic morphology identical to ours for SHA, but a microscopic morphology more closely resembling that of CAA. The difference is not understood. Depth profiling of the SHA oxide by SAM (see below) shows that the oxide is ~40-nm thick in the flat areas. Although we were unable to obtain a suitable cross-sectional sample for TEM analysis, selected area electron diffraction of planar TEM specimens shows that the SHA oxide is amorphous.

The PJ oxide surface contains relatively little microscopic roughness, as shown in Figures 2e and f. The oxide was very thin—on the order of 5–7 nm, which is consistent with earlier results.[10]

The morphology of CAA coupons was reported earlier for exposures in vacuum at temperatures up to 450°C for up to 160 hours (1200 hr in air at 330°C).[11] No changes were observed for vacuum exposures; air-exposure resulted in a slight thickening of the CAA cell walls. Identical results were obtained for

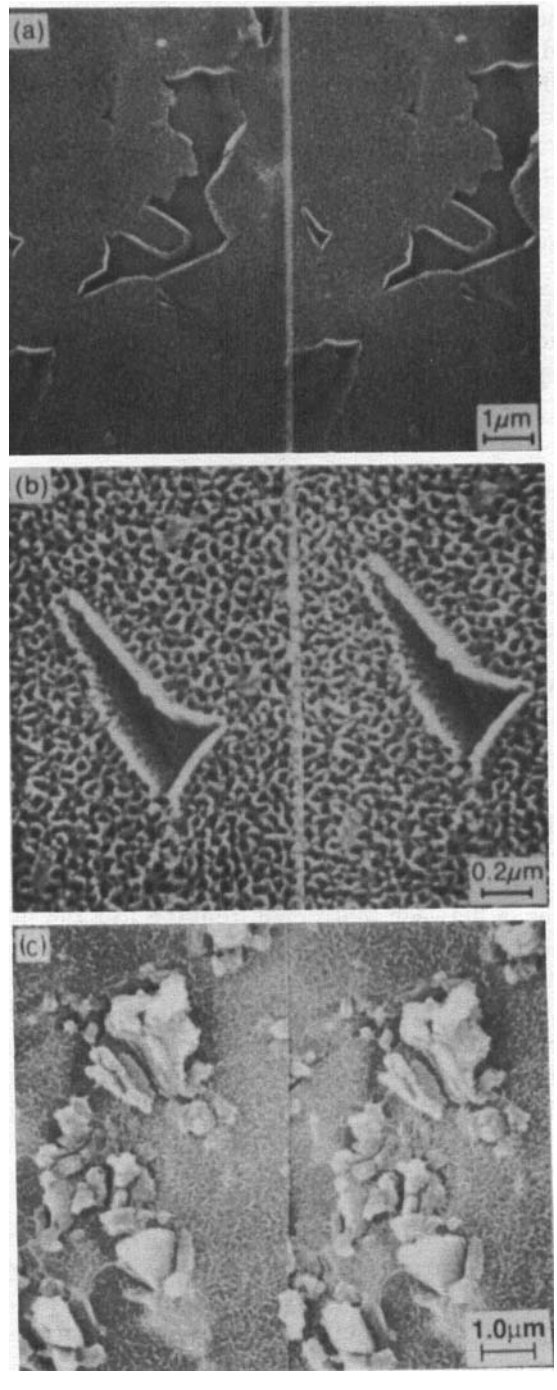

FIGURE 2 High-resolution scanning electron micrographs of the oxide suface preparations for Ti-6Al-4V: a) and b) chromic acid anodization; c) and d) sodium hydroxide anodization; and e) and f) Pasa-Jell 107.

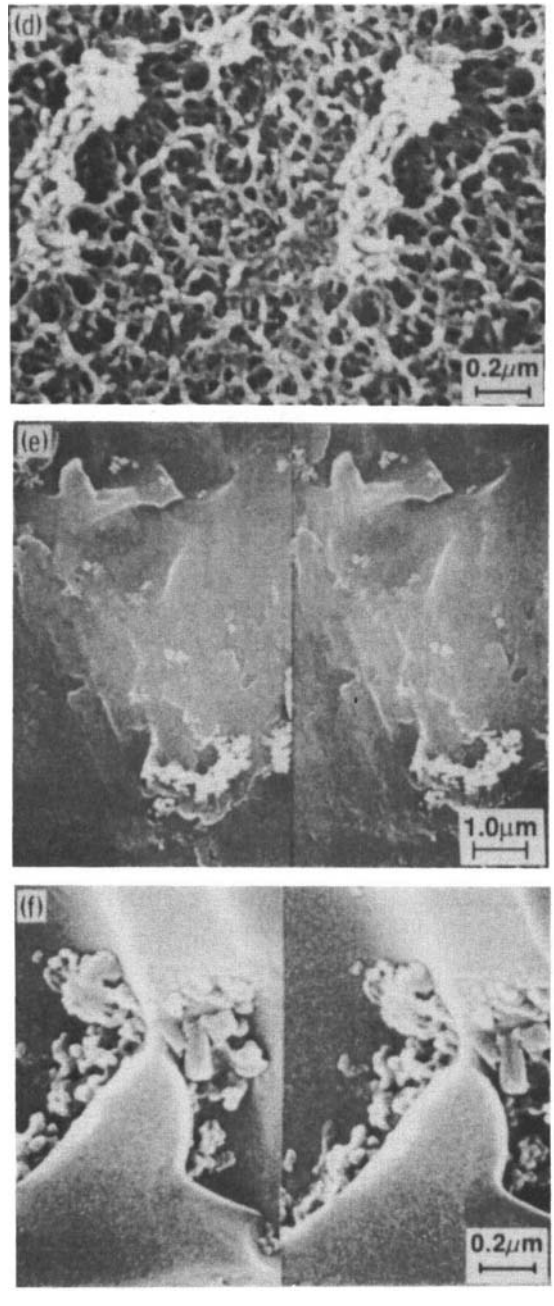

FIGURE 2 (*Continued.*)

SHA[24] and for PJ adherends exposed in vacuum. SHA adherends were also exposed to air at 330°C for 165 hr, with no change in morphology.

The bond strengths for the three adherends, both as-prepared and exposed, and both thin and thick, under most of the conditions described above, are presented in Table I. The differences in strength between thin and thick can be attributed mainly to varying degrees of adherend flexing during testing. Therefore, the tensile strength values are not used as an absolute indication of bond strength. However, the values can be used for relative comparisons between surface preparations or between as-prepared and exposed specimens because the results are reproducible to within 10%. The failure surfaces were examined as described above (results for CAA surfaces are shown in Ref. 11) and the loci of failure are indicated in parentheses in Table I. As we will demonstrate, this tensile test is also capable of reproducing bond failures observed by others.

The as-anodized CAA and SHA specimens consistently exhibited the highest bond strengths for both thin and thick adherends. Upon visual examination, both debonded surfaces had the same appearance, mainly that of the cured adhesive. This was confirmed by SEM and XPS analysis, which showed the characteristic morphology and atomic concentration of the cured adhesive on both failure surfaces. The tensile strength values then represent the cohesive strength of the adhesive for the particular adherend tested. The as-treated PJ adherends always exhibited less strength than the CAA or SHA adherends. The failure mode for the PJ specimens was mixed—cohesive and adhesive, which differs from the results obtained by Progar *et al.*,[1,2,23] who reported a cohesive failure mode for room-temperature lap shear tests of PJ-treated Ti-6Al-4V adherends bonded with

TABLE I
Tensile strength for CAA, SHA, and PJ adherends in the geometry of Ref. 11, for 0.08- and 0.28-cm-thick specimens

Exposure	Pull strength (MPa) Thickness		Failure mode
	0.08 cm	0.28 cm	
CAA			
as-anodized	9.2 ± 0.5	23.4 ± 1.2	cohes
air, 330°C			
160 hr	3.5	—	mixed cohes/oxide
1200 hr	<0.7	—	oxide
vacuum, 400°C			
24 hr	<0.7	1.0–2.7	oxide
SHA			
as-anodized	9.1	22.6	cohes
air, 330°C			
160 hr	6.7	—	mixed cohes/oxide
vacuum, 400°C			
24 hr	4.7	13.4	mixed cohes/oxide
PJ*			
as-etched	—	10.1	mixed adhes/cohes
vacuum, 200°C			
1 hr	—	2.5	oxide

* Values obtained in a separate study, see Fig. 6.

polyimide (thermoplastic) adhesives. The PJ adherends were not subjected to the same environmental exposures as the CAA and SHA adherends because we were unable to obtain 100% cohesive failures with them.

As reported earlier, the CAA adherends lost nearly all of their bond strength when exposed in vacuum at temperatures of 400°C for 24 hr or more.[11] We attributed that observation to either a stress buildup at the oxide-metal interface (due to differences in thermal expansion coefficient) or a change in the alloy microstructure. Subsequent investigations suggest that a more plausible explanation is dissociation of the oxide with subsequent dissolution of the oxygen into the adherend (by diffusion) at these temperatures and exposure times. This is shown in Figures 3a-c, which are Auger sputter-depth profiles of as-anodized (Figure 3a)

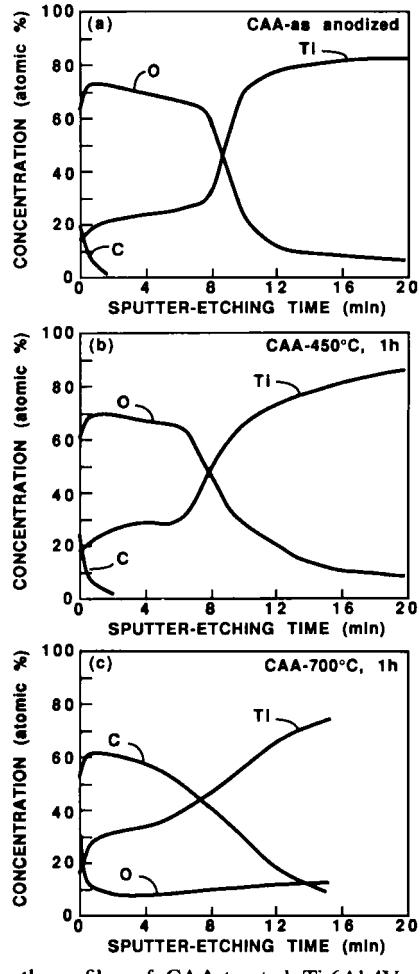

FIGURE 3 AES sputter-depth profiles of CAA-treated Ti-6Al-4V adherends after various exposures in vacuum: a) as anodized, b) 450°C for 1 hour, and c) 700°C for 1 hour. The etch rate is ~15 nm/min.

CAA surfaces and those heated in vacuum at 450 and 700°C for 1 hr. The etching rate in all three was ~15 nm/min. The as-anodized adherend exhibits a relatively sharp interface at a depth of ~130 nm. After 1 hr at 450°C (Figure 3b), the oxygen has begun diffusing into the alloy, as seen by the degradation of the original interface (*i.e.*, the "tail" on the O signal). This interfacial degradation becomes more pronounced at longer times or higher temperatures until, at 700°C, no oxide is found at the surface (Figure 3c). The oxygen present is probably due to adsorbed contaminants. Immediately below the surface, the oxygen concentration is nearly constant and is relatively close to the solubility limit in the alloy. For pure Ti, this is ~25 atomic%[36] but would be somewhat less for the alloy.[37] In addition, high carbon levels persist to a depth of 150 nm. This can be attributed to the formation of a carbide phase (see below).

Visual and SEM examination of the adherends support the oxide dissociation and oxygen dissolution processes. Initially, the CAA adherends exhibit a characteristic greenish-gold color due to optical interference between the oxide-air and oxide-metal interfaces. As the adherends are annealed to higher temperatures (1-hr exposure), the color changes—blue at 450°C, purple at 550°C, and clear at 650°C and above—which corresponds to progressively thinner oxides, with the lack of color indicating thicknesses less than ~20 nm. The characteristic CAA morphology is retained after 450°C exposure, but some change is evident after 500°C exposure, and after one hour at 700°C, all micro-roughness due to the CAA treatment is lost. Instead, the surface exhibits a "scaly" morphology, which we attribute to the surface carbide phase. The morphology after 700°C exposure is shown in Figure 4.

Although the tensile strength values listed in Table I suggest that SHA and PJ adherends do not degrade as severely as CAA surfaces, we have also observed oxygen dissolution in both. This is shown in Figures 5 and 6. The as-anodized SHA surface (Figure 5a) has a sharp oxide-metal interface in the flat areas at a depth of ~44 nm. After exposure at 500°C for 1 hour (Figure 5b), the interface is not as sharp and there is a considerable concentration of dissolved oxygen in the alloy (some interfacial degradation can be observed at temperatures as low as 330°C for SHA adherends). In this case, the high concentration of oxygen may arise from the mountainous features, whose composition we were unable to determine, or from the SHA oxide itself. After 700°C exposure, the depth profile resembles that obtained from the CAA surface exposed similarly, *i.e.*, oxygen dissolved to concentrations approaching the solubility limit and a surface carbide phase. The as-treated PJ adherend has a very thin oxide (Figure 6a) that actually grows with high-temperature exposure, as seen in Figure 6b. In this case, a vacuum of 3×10^{-4} Pa is apparently insufficient to prevent further oxidation of the Ti-6Al-4V adherend and the PJ oxide itself apparently is non-passivating.

To determine whether oxide failures occur in SHA and PJ adherends, several coupons of both (as well as CAA coupons for controls, were prepared and annealed simultaneously, *i.e.*, one coupon of each preparation, for one hour in the vacuum furnace at temperatures ranging from 300–900°C. The results of

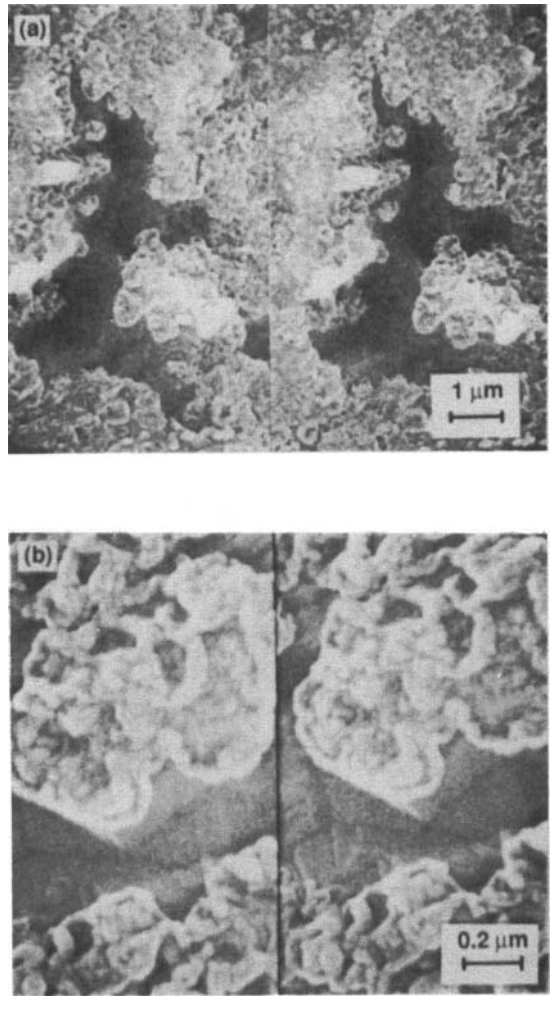

FIGURE 4 High-resolution scanning electron micgrographs obtained from a CAA-treated Ti-6Al-4V surface after exposure in vacuum at 700°C for 1 hour: a) low and b) high magnification.

subsequent tensile testing are shown in Figure 6. In each bond strength *vs* temperature curve, a minimum is observed. Analysis of the failure surfaces shows that, in all three cases, predominantly oxide failures occur at temperatures were the minimum bond strength is obtained. Because the coupons were positioned along the length of the quartz tube for simultaneous exposure, the temperatures shown in Figure 7 are nominal. We have subsequently determined that the temperature can vary by as much as 100 degrees along the tube, and specimen positions were not recorded. Thus, some differences occur between values shown

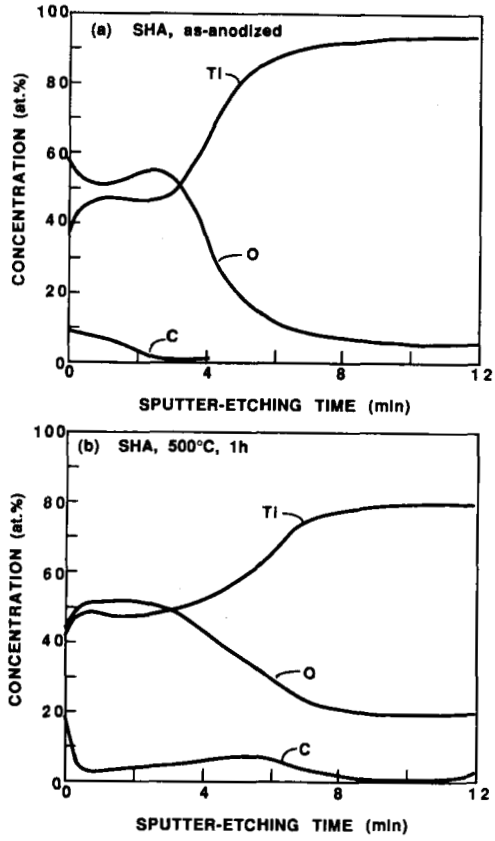

FIGURE 5 AES sputter-depth profiles of SHA-treated Ti-6Al-4V adherends: a) as-anodized; b) vacuum exposed, 500°C for 1 hour. The etch rate is ~15 nm/min.

in Figure 7 and those reported in Table I, particularly for the CAA-treated adherends. These are not significant, however, because the exposure times differed for the two experiments.

For all three surface treatments, the minimum bond strength corresponds to the onset of oxide dissociation as determined by sputter depth profiles. In the initial stages, oxygen dissolution into the alloy can have two deleterious effects on bond performance. Firstly, the oxide itself would be nonstoichiometric and most likely contain defects that would weaken it. Secondly, oxygen dissolved in the alloy at concentrations as low as 0.1 to 1 atomic% results in a highly-embrittled zone[34,37,38] just under the oxide-metal interface. Such an embrittled layer would have reduced fracture toughness. Either of these effects or the two combined could result in tensile failures under very little force.

As seen in Figure 7, all three adherends recover a significant fraction of their bond strength as the temperature is increased. High-resolution XPS suggests that this can be attributed to some degree to the formation of a carbide phase at the

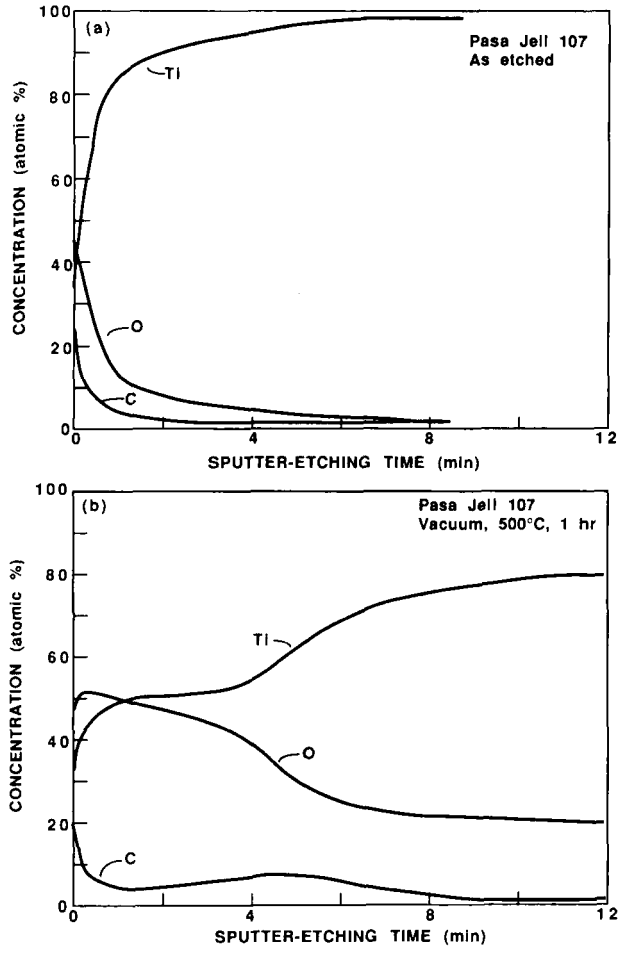

FIGURE 6 AES sputter-depth profiles of PJ-treated Ti-6Al-4V adherends: a) as-etched and b) vacuum exposed, 500°C for 1 hour. The etch rate is ~15 nm/min.

surface. This is shown in Figure 8. The three lower curves are the C, Ti, and O spectra for the typical, as-anodized CAA surface: the C 1 s spectrum results primarily from contaminants adsorbed during transfer to the analysis chamber; the Ti 2p spin-orbit split doublet represents a single chemical state, TiO_2; and the O 1 s spectrum is dominated by a metallic oxide state with a small amount of adsorbed contaminant. The three upper curves in Figure 8 were recorded after exposure in vacuum at 700°C. Their most significant feature is the development of new chemical states at lower binding energies in the C 1s and Ti 2p spectra. The C 1s peak at 281.4 eV and the Ti $2p_{3/2}$ peak at 454 eV are characteristic of TiC. In addition, for the O 1s spectrum, the ratio of metallic to contaminant oxide has changed dramatically, which is consistent with oxide dissociation at this temperature. The source of the carbon is likely to be CO, which typically is the major

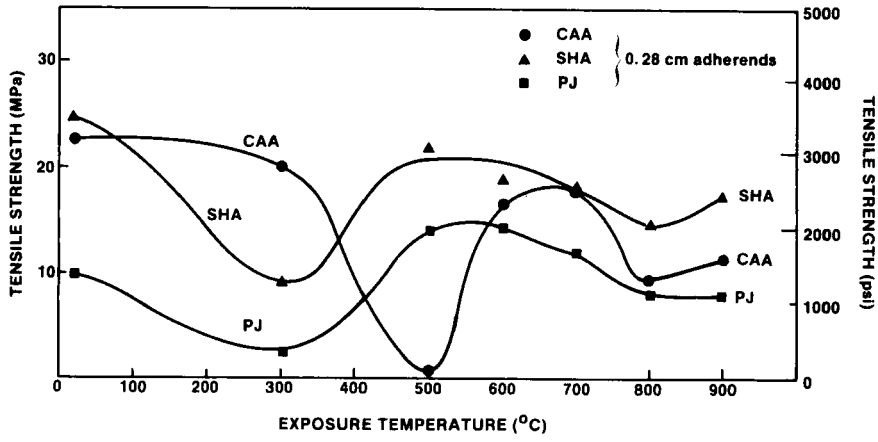

FIGURE 7 Tensile strength of Ti-6Al-4V adherends as a function of exposure temperature in vacuum. All exposures were 1 hour and specimens were bonded after exposure. The minimum in each curve corresponds to an oxide failure mode.

constituent in a vacuum ambient. Even at a partial pressure of 1.3×10^{-4} Pa, enough CO would react with the (now "metallic") Ti-6Al-4V surface during the 1-hr exposure to form a thin carbide layer. We have also observed this at lower temperatures over longer exposure times. This is significant because an adhesive in contact with a metallic Ti alloy surface at high temperature could potentially

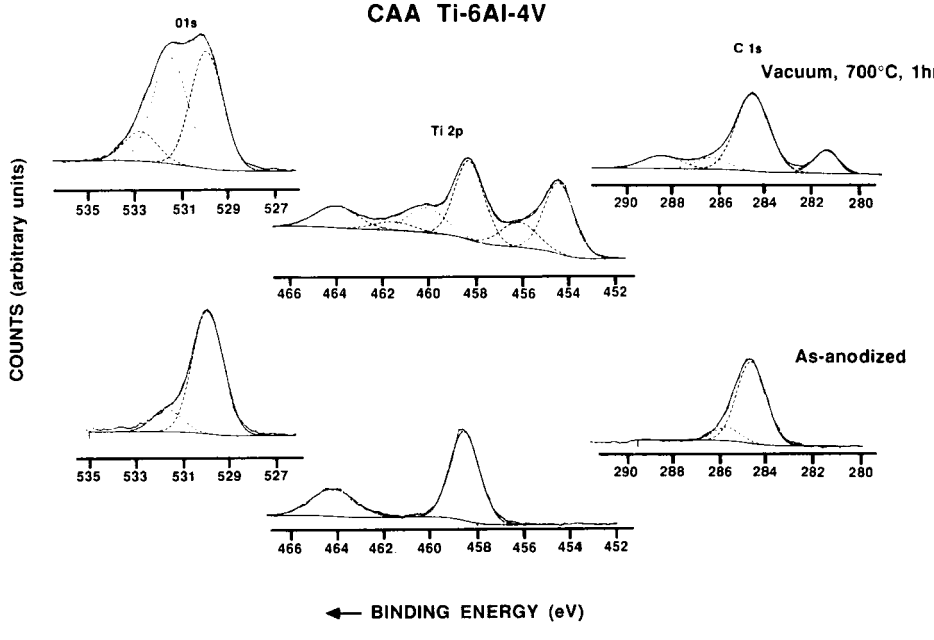

FIGURE 8 High-resolution XPS spectra of the O 1 s, Ti 2p, and C 1 s bound states obtained from CAA-treated Ti-6Al-4V adherends: bottom curves, as anodized; top curves, vacuum exposure for 1 hour at 700°C.

dissociate, with subsequent dissolution of the constituent elements into the alloy, thus resulting in bond failure.

Our investigation of oxide dissociation and carbide formation has been limited to temperatures above 300°C. In earlier studies, the long-term durability of Ti-6Al-4V bonds was investigated for aging at 232°C.[2,3,6] In those tests, the bonds were formed with polyimides (and other high-temperature resins) in the lap-shear configuration. Exposure times were on the order of 20,000 hr. In one study, Progar found that CAA adherends lost most of their strength after ~8000 hr.[2] SHA adherends also exhibited a loss of bond strength, but after ~13,000 hr.[2] Analysis of some of the SHA-treated specimens revealed failures in the oxide,[39] consistent with our accelerated tensile test results. In subsequent investigations, Progar *et al.* determined that PJ adherends are the most durable for lap shear specimens,[23] which suggests that they are least sensitive to oxide dissociation. The different dissociation or dissolution kinetics of the three surfaces are not understood at present, although the dissolution rate might be related to the initial oxide thickness[40] or the nature (*i.e.*, density or structure and, hence, passivity) of the barrier layer. However, we conclude that oxygen dissolution into the Ti-6Al-4V alloy can occur at temperatures below 300°C over long exposure periods. Hence, oxide surface preparations might be unsuitable for long-term service in high-temperature environments.

B. Plasma-sprayed adherend morphology and tensile tests

Micro-rough Ti-6Al-4V adherend morphologies can be obtained quite readily with plasma-sprayed (PS) Ti-6Al-4V coatings by properly controlling the deposition parameters. The micro-rough morphology produced by plasma spraying is different from any of the oxide morphologies, as seen in Figure 9. At the highest magnification, the micro-roughness is more random than any other adherend surface that we have examined. The pores are quite deep, and many knob-like protrusions can be seen. These protrusions result from the splat cooling and solidification of the Ti-6Al-4V droplets as they strike the substrate. At lower magnifications, some macroscopic inclusions are evident. According to SAM investigation, most are Ti alloy, presumably from droplets that cooled and solidified prior to striking the substrate. Like the oxide surfaces, the PS surface exhibits no change in morphology after exposure in vacuum at 450°C.

Tensile test results for the PS adherends are shown in Table II. As a control, we prepared a set of CAA specimens that were exposed concurrently with the PS specimens. Neither the thin or the thick PS adherends exhibited any significant loss in bond strength as a result of exposure. For the thick adherends, bond failure was always cohesive within the adhesive and the tensile strength was identical to that obtained for the as-anodized CAA adherends. The failure mode for the thin adherends was at least 95% cohesive within the adhesive. For these specimens, we occasionally observed some removal of the coating, most likely due to flexing of the adherend. The as-anodized (unexposed) CAA adherends failed within the adhesive, as expected. However, they exhibited oxide failures

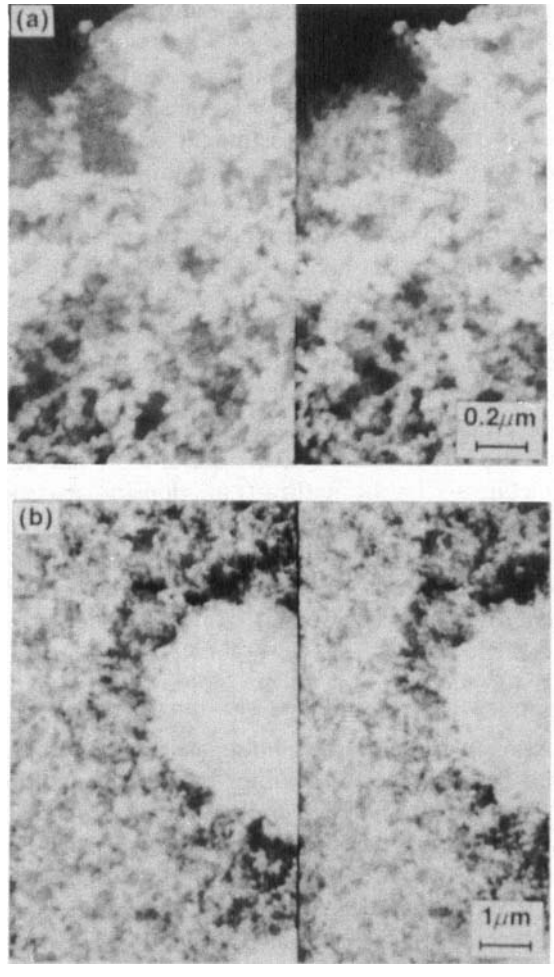

FIGURE 9 High-resolution scanning electron micrographs obtained from a plasma-sprayed Ti-6Al-4V surface. Note the random microscopic roughness: a) high and b) low magnification.

under very little tensile force for both elevated temperature exposures, consistent with results presented in Table I.

C. Durability testing

The simple tensile test above has been used as a screening procedure in choosing candidate surface preparations for durability testing. Performance and durability were determined on CAA-, SHA- and PS-treated adherends by the wedge/crack propagation test. PJ-treated adherends were not used because we were unable to obtain (100%) cohesive failures in the tensile test. For comparison, an additional set of panels was prepared by grit blasting alone.

TABLE II
Adhesion tensile test results for PS and CAA adherends exposed simultaneously

Exposure	Pull strength (MPa) Thickness		Failure mode
	0.08 cm	0.28 cm	
PS			
as-prepared	9.4 ± 0.5	23.4 ± 1.2	cohesive
vacuum, 450°C			
3 hr	8.5	—	cohesive
24 hr	8.6	20.6	cohesive
165 hr	8.6	20.9	cohesive
CAA			
as-anodized	9.2	23.4	cohesive
vacuum, 450°C			
3 hr	<0.7	2.8	oxide
24 hr	<0.7	<0.7	oxide

The wedge test results are shown in Figure 10. The CAA, SHA, and PS adherends performed identically within the error bars. We attribute the larger error in the CAA data to scatter in the initial crack lengths—all CAA specimens exhibited nearly identical crack propagation values, *i.e.*, 7–10 mm. For all three surface preparations, the final crack lengths are almost identical and nearly constant, suggesting that crack arrest occurs for all three in this particular test geometry. The crack propagation values conflict with those reported by Filbey *et*

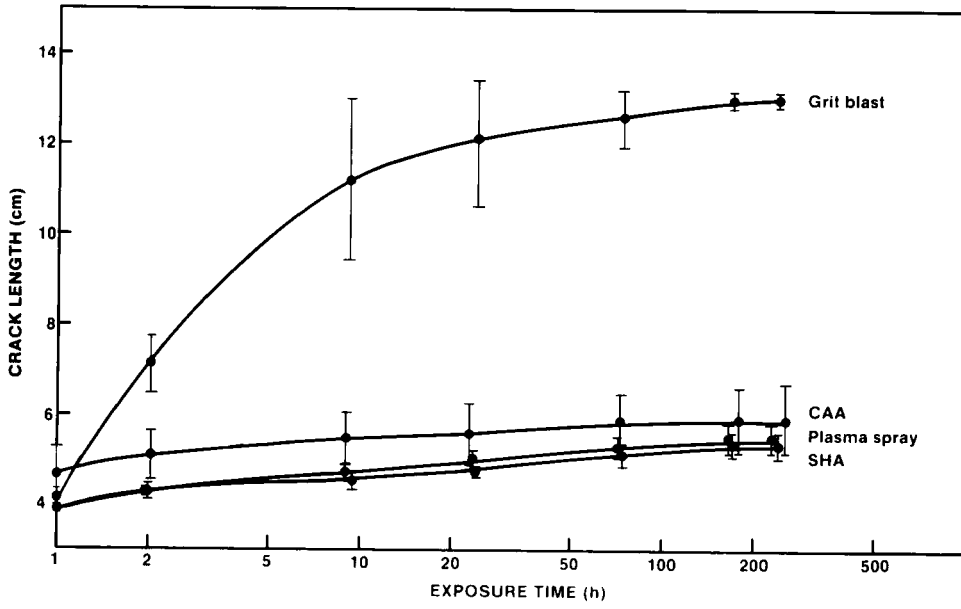

FIGURE 10 Crack length *vs.* exposure time for Ti-6Al-4V adherends bonded with FM-300M epoxy and immersed in boiling water. The performance of CAA, SHA and PS adherends is comparable.

al.,[14] who observed no crack propagation during similar environmental exposure. However, Filbey *et al.* might have used FM-300U, which does not contain a carrier cloth. Thus, the difference could be explained because an unsupported adhesive might be tougher than a supported one (water uptake will certainly be different). Our results are in agreement with those obtained for CAA adherends by Brown,[7] who used various epoxy and primer formulations.

The grit-blasted adherends performed much worse than the other three in the durability test. Most debonded completely within 24 hr. Because the wedge is 2.5 cm long, the maximum crack length is limited to 13 cm. The error bars in Figure 10 decrease in size over time as the crack lengths approach the maximum value. Those grit-blasted specimens that survived the test could be separated by hand.

The locus of failure for each of the adherends was determined by XPS. For this, spectra were recorded from both failure surfaces within 0.5 mm of the crack tip. Although the CAA, SHA, and PS adherends exhibited nearly identical crack propagation values, the loci of failure were different. For CAA adherends, crack propagation occurred entirely within the adhesive, *i.e.*, the failure was cohesive. However, for the SHA and PS adherends, the locus of failure changed during the test. The crack propagated initially (before exposure) through the adhesive but, during exposure, switched almost immediately to propagation between the adhesive and the adherend. The locus of failure for the grit-blasted specimens was identical to that for the SHA and PS adherends.

The similarity in locus of failure between the PS and grit-blasted specimens is significant. Unbonded witness specimens of each (as-treated) were analyzed by XPS, which showed them to be TiO_2; the only difference between them, within our ability to distinguish, is in the morphology. The PS surfaces (Figure 9) exhibit significant micro-roughness, whereas the grit-blasted surfaces, shown in Figure 11, do not. Assuming that any chemical bonding that exists between the metal surface and the adhesive for both specimens is disrupted or displaced by water, then the difference in crack propagation rates can be attributed to a micromechanical interlocking between the adhesive and the adherend. In this case, the crack propagation in the first 10 hr (7 cm for grit blast *vs* ~ 0.6 cm for PS) is slowed by at least an order of magnitude by the presence of the micro-rough morphology.

Chemical interactions may further enhance the bond durability of a stable, micro-rough adherend. This has been demonstrated in wedge/crack-propagation results reported by Ahearn and Davis for Forest Products Laboratory (FPL) treated 2024 Al adherends that were chemically altered by adsorption of various hydration inhibitors.[41,42] The crack growth rate and locus of failure depended on the interaction between the inhibitor and the adhesive even though the morphology was constant. Such a chemical interaction could explain the difference in failure mode between our CAA and SHA specimens. Both surfaces exhibit significant micro-roughness albeit not to the same degree. Filbey *et al.* determined that the CAA surface had a residual pH < 6 and that the SHA surface had a residual pH > 8.[14] Results shown here suggest that water can displace the oxide-adhesive bond more readily for SHA specimens. The combination of our

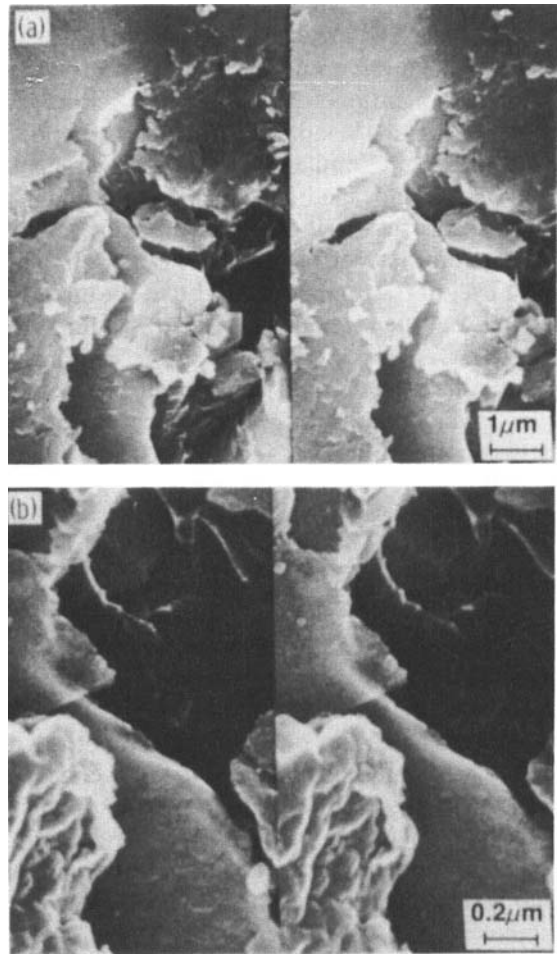

FIGURE 11 High resolution scanning electron micrographs obtained from a grit-blasted Ti-6Al-4V adherend surface: a) low and b) high magnification. The surface is devoid of microscopic roughness.

results with those of Filbey *et al.*[14] suggests that an acid-base interaction, similar to that proposed by Fowkes,[43] might be a contributing factor in bond durability.

During the course of the durability test, we noted a swelling of the adhesive and an increase in bondline thickness for some distance ahead of the crack tip. The adhesive appeared "spongy" in the swelled region, suggesting that water was present in liquid form at the bondline. Although the intended service environment includes exposure to moisture and jet engine fuel at ambient temperatures, the bondline will experience prolonged exposure at 232–400°C, at which water and other solvents will be present only as vapor. Thus, a durability test conducted with an epoxy adhesive in a medium such as boiling water may not be indicative of the potential performance of the PS adherends at high temperatures.

In addition, a polyimide or similar adhesive will be used for the bonded structure.[1–3] Such adhesives require cure temperatures near 400°C and high pressures. We believe that PS adherends will significantly outperform the others under these conditions. As mentioned above, Progar observed (oxide) failures in CAA- and SHA-treated Ti-6Al-4V lap shear specimens bonded with a polyimide adhesive and aged at 232°C.[1–2] Similar observations were made by Peters and coworkers on CAA-treated and aged specimens.[3,6] Although the PS adherends contain a native oxide, dissociation of such an oxide might not be severely detrimental to high-temperature performance. The oxide might dissociate completely during the cure cycle at a temperature above the glass transition temperature of the adhesive. At such temperatures, the adhesive should flow and penetrate the micro-rough coating so that, upon cooling, the adhesive will establish chemical and micro-mechanical bonds with the metallic surface. Even if the chemical bonding is disrupted during high-temperature service, the mechanical interlocking between the adhesive and the coating should be sufficient to maintain bond strength.

NOTE ADDED AFTER REVIEW

We have completed preliminary wedge/crack durability testing of both CAA- and PS-treated Ti-6Al-4V structures that were bonded with LaRC-TPI and cured at 400°C for 1 hour. Several of the CAA specimens debonded completely during insertion of the wedge. In these, the failure occurred entirely at the oxide-metal interface. Those CAA specimens that survived the wedge test exhibited crack propagation that was predominantly between oxide and metal, with small areas of cohesive failure. The PS specimens all exhibited crack propagation that was entirely cohesive within the adhesive. In addition, strain energies (*i.e.*, G_1) calculated at the end points of the test for the PS specimens are ~4–5 times those for the CAA specimens.

IV. SUMMARY AND CONCLUSIONS

We have investigated the bond strengths of Ti-6Al-4V adherends prepared by CAA, SHA, PJ 107 etching, and a new treatment, a plasma-sprayed Ti-6Al-4V coating, as a function of (pre) expsoure to high-temperature, dry environments. This was accomplished by using a simple tensile test designed to provide a relative indication of the integrity of the oxide (or coating)/metal interface. Although the as-anodized adherends provided maximum bond strength with cohesive failures, they and the PJ adherends exhibited oxide failures after high-temperature exposure (although at different temperatures). The mechanism responsible for the oxide failures is dissociation of the oxide with subsequent dissolution of oxygen into the alloy, which results in a nonstoichiometric oxide and a highly embrittled zone in the alloy. The weakest bond strengths were obtained at the

onset of this process. The PS-treated adherends exhibited cohesive failures (within the adhesive) regardless of the exposure. In addition, their ability to arrest crack growth in the wedge test used here (epoxy adhesive, boiling water) is nearly comparable with that of the CAA-treated adherends.

The simple tensile test used in this study reproduces actual failures observed in structures bonded with high-temperature resins although it does not provide a quantitative estimate of bond strength. It is a viable screening procedure for the surface preparation of metals because it can be accomplished quickly and with a minimum of consumed material.

The plasma spray process is also applicable to bonding of adherends other than titanium alloys. Any material that can be obtained in powder form can be plasma sprayed. Thus, one can envision preparing steel and aluminum adherends with coatings that are more environmentally-stable than those used at present. In addition, the spraying process can be highly automated so that odd-shaped structures can be coated. This should have tremendous benefit in the design and production of advanced aerospace structures, particularly for those applications where extended high-temperature durability is important.

Acknowledgements

This work was supported by the Office of Naval Research under contract no. N00014-85-C-0804. We have had many useful discussions with Martin Marietta personnel including J. D. Venables, G. D. Davis, C. O. Arah, D. Nagle, and D. K. McNamara as well as others including J. C. Williams, T. L. St. Clair, D. J. Progar, K. M. Liechti and J. P. Wightman. G. O. Cote and K. A. Olver acquired much of the XPS and SAM data, respectively, and M. E. Marousek assisted with the plasma spraying. We are grateful to D. Progar for providing lap shear specimens for failure analysis and to American Cyanamid for providing the FM-300M adhesive. The assistance of A. Paskun and A. Kovensky in the preparation of the manuscript is appreciated. One of us (H.M.C.) is grateful to the organizers of the 35th Sagamore Army Materials Research Conference for the invitation to present this material.

References

1. D. J. Progar and T. L. St. Clair, *J. Adhesion* **21,** 35 (1987).
2. D. J. Progar, *J. Adhes. Sci. Technol.* **1,** 135 (1987).
3. P. D Peters, E. A. Ledbury, C. L. Hendricks and A. G. Miller, in *Proc. 27th Natl. SAMPE Symposium* (SAMPE, Azusa, CA, 1982), p. 940.
4. Y. Moji and J. A. Marceau, *Method of anodizing titanium to promote adhesion,* U.S. Patent No. 3959091 (1976).
5. J. D. Venables, *J. Mater. Sci.* **19,** 2431 (1984).
6. S. G. Hill, P. D. Peters, and C. L. Hendricks, NASA contractor report 177936, under contract no. NAS1–15605, 1985 (unpublished).
7. S. R. Brown, in *Proc. 27th Natl. SAMPE Symp.* (SAMPE, Azusa, CA, 1982), p. 363.
8. B. M. Ditchek, T. I. Morgenthaler, T. S. Sun and R. L. Hopping, in *Proc. 25th Natl. SAMPE Symp.* (SAMPE, Azusa, CA, 1980), p. 909.
9. R. F. Wegman and D. W. Levi, in *Proc. 27th Natl. SAMPE Symp.* (SAMPE, Azusa, CA, 1982), P. 440.
10. M. Natan, J. D. Venables, and K. R. Breen, in *ibid.* (SAMPE, Azusa, CA, 1982), p. 178.
11. H. M. Clearfield, D. K. Shaffer, J. S. Ahearn and J. D. Venables, *J. Adhesion* **23,** 83 (1987).
12. J. A. Skiles and J. P. Wightman, Virginia Polytechnic Institute and State University Report under contract N00014-82-K-0185 (Office of Naval Research), 1986.
13. A. C. Kennedy, R. Kohler and P. Poole, *Int. J. Adhes. and Adhesives* **3,** 133 (1983).

14. J. A. Filbey, J. P. Wightman, and D. J. Progar, *J. Adhesion* **20,** 283 (1987).
15. C. Matz, *Int. J. Adhes. and Adhesives* **8,** 17 (1988).
16. K. W. Allen, H. S. Alsalim and W. C. Wake, *J. Adhesion* **6,** 153 (1974).
17. J. L. Cotter and A. Mahoon, *Int. J. Adhes. and Adhesives* **2,** 47 (1982).
18. A. Mahoon, in *Proc. 27th Natl. SAMPE Symp.* (SAMPE, Azusa, Ca, 1982), p. 150.
19. A. K. Rogers, K. E. Weber and S. D. Hoffer, in *ibid.* (SAMPE, Azusa, CA, 1982), p. 63.
20. M. E. Schrader and J. A. Cardamone, J. *Adhesion* **9,** 305 (1978).
21. F. J. Boerio and R. G. Dillingham, in *Adhesive Joints, Formation, Characteristics and Testing,* K. Mittal, Ed. (New York, Plenum, 1984), p. 541.
22. Pasa Jell 107 is a trademark of Semco, Inc., Glendale, CA.
23. D. J. Progar, *J. Adhes. Sci. Technol.* **1,** 53 (1987).
24. D. K. Shaffer, H. M. Clearfield, C. P. Blankenship, Jr. and J. S. Ahearn, in *Proc. 19th Intl. SAMPE Tech. Conf.* (SAMPE, Azusa, CA, 1987), p. 291: H. M. Clearfield, D. K. Shaffer, C. P. Blankenship, Jr. and J. S. Ahearn, in *Proc. 5th Joint Military/Government/Industry Symposium on Structural Adhesive Bonding* (ADPA, Arlington, VA, 1987), p. 206.
25. H. D. Steffens, E. Erturk and K. H. Busse, *J. Vac. Sci. Technol.* **A3,** 2459 (1985).
26. J. D. Ayers, R. J. Schaefer, F. D. Bogar and E. McCafferty, *Corrosion* **37,** 55 (1981).
27. I. S. Gel'tman, N. V. Rogov and V. I. Pankov, *Sov. J. Frict. Wear* **6,** 136 (1986).
28. H. Hahn, P. J. Jare, R. H. Rowe, Jr., A. C. Fraker and F. Ordway, in *Corrosion and Degradation of Implant Materials: Second Symposium,* A. C. Fraker and C. D. Griffin, Eds. (ASTM, Philadelphia, 1985), p. 179.
29. A. J. Kinloch, *Adhesion and Adhesives: Science and Technology* (Chapman and Hall, London, 1987).
30. H. M. Clearfield, D. K. Shaffer and J. S. Ahearn, in *Proc. 18th Intl. SAMPE Tech. Conf.* (SAMPE, Azusa, CA, 1986), p. 921.
31. Scotchbrite is a trademark of 3M Co., St. Paul, MN.
32. P. A. Redhead, J. P. Hobson and E. V. Kornelsen, *The Physical Basis of Ultrahigh Vacuum* (Chapman and Hall, London, 1968).
33. H. M. Clearfield, G. O. Cote, K. A. Olver and J. S. Ahearn, *Surf. Interface Anal.* **11,** 347 (1988).
34. A. M. Chaze and C. Coddet, *Oxidation of Metals* **28,** 61 (1987); C. Coddet, A. M. Chaze and G. Beranger, *J. Mater. Sci.* **22.** 2969 (1987).
35. M. Natan and J. D. Venables, *J. Adhesion* **15,** 125 (1983).
36. F. A. Shunk, *Constitution of Binary Alloys, Second Supplement* (McGraw-Hill, New York, 1969).
37. A. M. Chaze and C. Coddet, *J. Mater. Sci.* **22,** 1206 (1987).
38. C. E. Shamblen and T. K. Redden, in *The Science, Technology and Application of Titanium,* R. I. Jaffe and N. E. Promisel, Eds. (Pergamon, Oxford, 1966), p. 199.
39. D. K. Shaffer and H. M. Clearfield, unpublished results.
40. C. Panagopoulos and H. Badekas, *Materials Letters* **5,** 307 (1987).
41. J. S. Ahearn and G. D. Davis, in *Proc. Adhesion '87* (York, England, 1987), p. 291.
42. J. S. Ahearn and G. D. Davis, *J. Adhesion,* in press.
43. F. M. Fowkes, *J. Adhes. Sci. Technol.* **1,** 7 (1987), and references therein.